IL NUOVO CIMENTO Vol. 26 C, N. 1 Gennaio-Febbraio 2003

Maximum downward propagation of the baroclinic wind-driven circulation into the ocean interior

F. Cavallini([1])([*]) and F. Crisciani([2])([**])

([1]) *Istituto Nazionale di Oceanografia e di Geofisica Sperimentale (OGS) Borgo Grotta Gigante 42/c, I-34010 Sgonico (TS), Italy*

([2]) *Istituto Talassografico del Consiglio Nazionale delle Ricerche (CNR) Viale Romolo Gessi 2, I-34123 Trieste, Italy*

(ricevuto il 7 Febbraio 2002; revisionato il 16 Dicembre 2002; approvato il 13 Gennaio 2003)

Summary. — In the framework of the Young and Rhines theory of the baroclinic, wind-driven circulation, we consider the problem of the determination of the maximum penetration depth, $D_{\max}$, of the motion into the ocean. On the basis of general results concerning the interface of no-motion $D(x, y)$, we investigate the dependence of $D_{\max}$ on a couple of parameters that select each buoyancy profile within a given class, having fixed a special family of vertical Ekman velocity fields. We also show some circulation patterns forced by a typical sinusoidal wind-stress and corresponding to different buoyancy profiles within the same class.

PACS 92.10.Fj – Dynamics of the upper ocean.

1. – Introduction

A very important task of theoretical oceanography is to explain, in terms of the principles of fluid mechanics, the downward propagation of horizontal motion into a ventilated ocean. This problem has been faced within different contexts since Ekman [1], Sverdrup [2], Charney [3] and also nowadays it is an active research field. In particular, the framework of the present investigation is the theory of Young and Rhines [4, 5], dealing with the wind-driven circulation of ocean gyres in a continuously stratified fluid, far from the western coast of a hypothetical reference basin. Their theory basically assumes the tendency to the conservation of quasi-geostrophic potential vorticity, which is the dynamical foundation of the model together with some special assumptions about the diffusion and dissipation of potential vorticity.

([*]) E-mail: fcavallini@ogs.trieste.it
([**]) E-mail: fulcri@itt.ts.cnr.it.

The implications of this model typically concern with the structure of the surface of no motion and the overall density distribution of a baroclinic ocean. We stress that, in the present context, an adiabatic ocean is understood; thus, the above features have a strictly mechanical genesis. The adopted quasi-geostrophic approximation at the basin scale assumes a background density field that acts as an input of the model and explicitly enters into the dynamics through the buoyancy frequency, which appears, in turn, into the thermal vorticity term.

The basic input of the model are the background density and the wind forcing over the ocean. In particular, once both the buoyancy frequency and the vertical Ekman velocity are given, this theory allows us to evaluate the maximum downward propagation $D_{\max}$ of the motion into the ocean interior. In the present investigation we focus our attention to $D_{\max}$. To this purpose, we introduce a two-parameter buoyancy-frequency profile that generalizes others taken into account in the literature and that is more suitable to fit observational data. Moreover, we assume that the vertical Ekman velocity satisfies some physically realistic properties within a class of functions of latitude, although it is not explicitly given. On this basis, we explore the dependence of $D_{\max}$ on the parameters appearing in the buoyancy profile, without any further hypothesis on the forcing. An interesting result is that, if the pycnoclyne is sufficiently close to the interface between the upper Ekman layer and the ocean interior, then $D_{\max}$ is independent of the typical depth of the pycnocline itself. Finally, we point out some solutions of the circulation problem, corresponding to different values of the buoyancy parameters and to the usual sinusoidal wind stress.

2. – Model equations

To define precisely the foundations of the present investigation, we shortly expound the core of the theory of Young and Rhines (see [4] and [5, sect. 3]), revisited also in Young [6] and in Pedlosky [7, sect. 3.10], concerning with wind-driven circulation in continuously stratified quasi-geostrophic oceans.

Main equation. In the subsurface flow and away from the western boundary layer, it is assumed that, first, the dissipation of vorticity is sufficiently weak to establish $O(1)$ free geostrophic modes beneath the ventilated layer; and, second, the inwards diffusion of potential vorticity is slow enough to lead to a uniform value inside each region enclosed by a streamline. Then, the basic governing equation for the unknown streamfunction $\psi(x, y, z)$ is the second-order linear nonhomogeneous ordinary differential equation

$$\frac{\partial}{\partial z}\left(\frac{1}{B(z)^2}\,\frac{\partial \psi}{\partial z}\right) = 1 - y \ , \tag{1}$$

where nondimensional quantities are understood. In (1) we have put $B(z) = N(h\,z)/N_0$, where N_0 is the characteristic scale of the buoyancy frequency (or Brunt-Väisälä frequency) $N(z_*) = N(z\,h)$, while $0 \le y \le 1$ is the nondimensional latitude in the square basin considered here. Every choice of $B(z)$ must be consistent with the following prescriptions:

$$B(0) = 1 \ , \tag{2}$$

and

$$\frac{\partial B}{\partial z} \geq 0 \ . \tag{3}$$

Equation (2) immediately comes from the scaling argument just seen, while (3) simply expresses the static stability of the fluid column.

The horizontal coordinates x and y are each confined in the interval (0, 1), while the vertical coordinate z is negative. The l.h.s. of (1) is the potential vorticity of the fluid column, say q, deprived of the (actually, very small) relative vorticity term $\nabla^2\psi$; and (1) itself comes from the approximate equation (where J is the Jacobian operator)

$$J(\psi,\, q) = 0 \ , \tag{4}$$

valid in the limit of a vanishing vorticity dissipation once homogenization has taken place. To explain the r.h.s. of (1), we recall that the subsurface flow develops along closed streamlines, also called closed contours, whose shape varies with depth. The contours, at each depth, are contiguous with the northern boundary of the gyre, located in $y = 1$, where the fluid column has only planetary vorticity. Thus, the conservation principle (4), together with the known value of q, *i.e.* $q = 1$ along the northern boundary, leads to the r.h.s. of (1).

Boundary conditions. The vertical boundary condition associated to (1), at the depth of the interface between the turbulent upper Ekman layer and the geostrophic interior, which we set in $z = 0$, has the form

$$w_{\mathrm{E}} = -J\left(\psi\,,\ \frac{\partial\,\psi}{\partial\, z}\right) \qquad \text{on} \quad z = 0 \ , \tag{5}$$

where $w_{\mathrm{E}}(x,\, y)$ is the current of the Ekman pumping. In (5) and similar equations below, we write "on" and not "at" because the condition $z = 0$ defines a surface in the $(x,\, y,\, z)$-space, and not a single point. Physically, the level $z = 0$ is 150–200 m below the free surface of the ocean.

We suppose that the quasi-geostrophic wind-driven circulation lies between the upper interface, $z = 0$, and the lower level of no motion, $z = -D(x,\, y)$. On this surface, the further boundary conditions are

$$\psi = 0 \quad \text{and} \quad \frac{\partial\,\psi}{\partial\, z} = 0 \qquad \text{on} \quad z = -D(x,\, y) \ . \tag{6}$$

Boundary conditions (6), together with the absence of motion in the region $z < -D(x,\, y)$, imply $\psi = 0$ there. Problem (1), (5), (6) is a "free" boundary value problem, since $D(x,\, y)$ must be determined in such a way as to satisfy the additional boundary condition (5).

To summarize, the problem is now the following. Given the nondimensional buoyancy profile $B(z)$ and the nondimensional vertical current $w_{\mathrm{E}}(x,\, y)$, find the stream function $\psi(x,\, y,\, z)$ and the interface of no-motion $z = -D(x,\, y)$ such that firstly, for $z > -D(x,\, y)$ the nondimensional model equation (1), which governs the interior flow, is satisfied and, secondly, also the boundary conditions (5) and (6) are fulfilled.

Finally, we note that the problem just stated may be formulated in "starred" (*i.e.* dimensional) variables by using the constants U, h and L that represent typical values of velocity, depth and horizontal length scale, respectively:

$$\psi = \frac{1}{U\,L}\,\psi_*\,, \qquad (x,\,y) = \frac{1}{L}\,(x_*,\,y_*)\,, \qquad z = \frac{1}{h} z_* \tag{7}$$

and by exploiting the Sverdrup balance to introduce the dimensional vertical velocity

$$w_* = \frac{\beta\,U\,h}{f_0}\,w\ , \tag{8}$$

where f_0 is the middle-basin Coriolis parameter and β is the planetary vorticity gradient.

3. – General results about the interface of no motion

The interface of no-motion $z = -D(x,\,y)$ separates the stratified and wind-driven fluid layer from the underlying one, which fills the remainig part of the ocean basin and stays at rest or is driven by different mechanisms. The details of the interface depend on the Brunt-Väisälä frequency $B(z)$ and on the input of the system, which is given by the Ekman vertical current $w_{\mathrm{E}}(x,\,y)$. Basically, two models for the buoyancy frequency are found in the literature: the constant profile $B(z) = 1$ and the exponential profile $B(z) = \exp[a\,z/2]$. In what follows we generalize the form of $B(z)$ to investigate the sensitivity of the circulation model (and, specifically, of the maximum penetration depth) in view of future applications to more realistic situations.

Solving for the stream function. The free boundary problem (1), (5), (6) is completely posed once w_{E} and $B(z)$ are assigned; however, we can state some general properties of $D(x,\,y)$ under rather general assumptions about the Ekman pumping and the buoyancy frequency. To this purpose, we integrate (1) with the aid of (6) to obtain

$$\frac{\partial\,\psi}{\partial\,z} = \begin{cases} (1-y)\,(z+D)\,B(z)^2 & \text{for} \quad z > -D(x,\,y)\,, \\ \\ 0 & \text{for} \quad z \le -D(x,\,y) \end{cases} \tag{9}$$

and then integrate (9), again with the aid of (6), to get: $\psi(x,\,y,\,z) = 0$ if $z \le -D(x,\,y)$, and

$$\psi(x,\,y,\,z) = (1-y)\left(\int_{-D(x,\,y)}^{z} \theta\,B(\theta)^2\,\mathrm{d}\theta + D(x,\,y)\int_{-D(x,\,y)}^{z} B(\theta)^2\,\mathrm{d}\theta\right) \tag{10}$$

if $z > -D(x,\,y)$.

Boundary condition. The boundary condition that $D(x,\,y)$ must satisfy, together with eq. (13) below, comes from the request that the zonal flow does vanish on the eastern boundary (*i.e.* $u \equiv -\partial\psi/\partial y = 0$ on $x = 1$). From (10) we evaluate

$$u = \int_{-D}^{z}\left(D - (1-y)\,\frac{\partial D}{\partial y} + \theta\right)\,B(\theta)^2\,\mathrm{d}\theta$$

and we see that

$$D(1,\, y) = 0\ , \tag{11}$$

because $u(1,\, y,\, z) = 0$ must hold. Note that, because of the inequality $-D \le z \le 0$, the fluid in motion has zero depth on the eastern boundary.

In the rest of this section, the dependence of D on y will always be understood, so the boundary condition (11) is simply rewritten as

$$D(1) = 0\ . \tag{12}$$

The interface between the moving and the motionless layer. As shown in the Appendix, the nondimensional Ekman vertical velocity may be expressed as

$$w_{\mathrm{E}} = (y-1)\,\Gamma(D)\,\frac{\partial D}{\partial x} \qquad \text{on } z = 0\ , \tag{13}$$

where, by definition,

$$\Gamma(D) \equiv \int_{-D}^{0} z\,B(z)^2\,\mathrm{d}z < 0\ . \tag{14}$$

We refer the circulation problem to a hypothetical subtropical gyre included between two latitude circles located in $y = 0$ and $y = 1$, respectively. We also assume that

$$w_{\mathrm{E}}(0) = w_{\mathrm{E}}(1) = 0\,, \tag{15}$$

$$w_{\mathrm{E}}(y) < 0 \quad \forall y \in]0, 1[\,, \tag{16}$$

$$w_{\mathrm{E}}(y) \text{ is a convex function in } [0, 1]\,, \tag{17}$$

$$\lim_{y\to 1} \frac{w_{\mathrm{E}}(y)}{1-y} < \infty\,. \tag{18}$$

We define $M = M(y) = -w_{\mathrm{E}}(y)/(1-y)$, so that $M(y) > 0$. Moreover, from the above listed features of $w_{\mathrm{E}}(y)$, it follows that $M(y)$ is an increasing function of y, which implies $M(y) \le M(1)$. Typical Ekman vertical velocities satisfying conditions (15)-(18) are obtained, for instance, from any of the following assumptions:

$$w_{\mathrm{E}}(y) \propto 2|y - \frac{1}{2}| - 1\,, \qquad w_{\mathrm{E}}(y) \propto -\sin(\pi\, y)\,, \qquad w_{\mathrm{E}}(y) \propto (y-1)\,y\,.$$

The first and second choices are discussed in the paper by Young and Rhines [5]. Without loss of generality, we normalize $w_{\mathrm{E}}(y)$ in such a way that

$$M(1) = 1\,. \tag{19}$$

As the dependence of D on y is only parametric, (13) may be rewritten as an ordinary differential equation:

$$\Gamma(D(x))\,\frac{\mathrm{d}D}{\mathrm{d}x} = M\ . \tag{20}$$

The integration of (20) with the aid of (12) yields

$$\Sigma(D) = (1 - x)\, M(y) \ , \tag{21}$$

where we have put, by definition,

$$\Sigma(D) \equiv \int_D^0 \Gamma(\tilde{D})\, \mathrm{d}\tilde{D} \ . \tag{22}$$

From (20) we immediately see that $\mathrm{d}D/\mathrm{d}x$ is a continuous function whenever $z\, B(z)^2$ is integrable. Further, it is easy to prove the concavity and monotonic decreasing behaviour of $D(x)$ (see Appendix).

The solution $D(x)$ of problem (20), (12) is unique (see Appendix). Physically, this means that the ocean reacts in a univocal way to the applied forcing w_{E}.

We may infer the local behaviour of $D(x)$ close to $z = 0$ under weak assumptions on $B(\theta)$. If we linearize $\theta\, B(\theta)^2$ about $\theta = 0$ (*i.e.* we use $\theta\, B(\theta)^2 = B(0)^2\, \theta$ in (20)), then the resulting differential equation for $D(x)$ is

$$D^2\, \frac{\mathrm{d}D}{\mathrm{d}x} = -2M \ ,$$

whose unique integral satisfying (12) is

$$D^3 = 6(1 - x)\, M(y) \ . \tag{23}$$

Profile (23) gives some insight into the circulation pattern in the easternmost area, for very small depths below the Ekman layer: to a large extent, it results to be independent on the background density distribution. Only if $B(z) = 1$ for all $z \leq 0$, eq. (23) holds in the whole longitudinal interval $0 < x \leq 1$. This case has been extensively analyzed by Young and Rhines [4,5] and Pedlosky [7].

An equation for the maximum penetration depth of the interface can be obtained as follows. Firstly, because of (14) and (22), $\mathrm{d}\Sigma/\mathrm{d}D > 0$ holds; so, (21) yields $\max \Sigma(D) = \Sigma(\max D)$. Secondly, recalling eq. (19) we have $\max[(1 - x)M(y)] = 1$. Hence the equation

$$\Sigma(D_{\max}) = 1 \tag{24}$$

holds and implicitly gives $D_{\max} = \max_{x,y} D(x, y)$.

4. – Wind-driven circulation

4˙1. *A family of buoyancy-frequency profiles.* – To evaluate $D_{\max}$ from (24), we need to know $B(z)$ in order to obtain Σ from (14) and (22).

As mentioned at the beginning of the preceding section, the two special forms of $B(z)$ most used in the literature are: the constant profile $B(z) \equiv 1$, and the exponential profile $B(z) = \exp[a\, z/2]$. The first is taken into account mainly because of its mathematical simplicity. The second gives a satisfactory best fit of measured data [8] and is also easily manageable in the computations. The presence of only one free parameter in the exponential buoyancy frequency makes its profile somewhat "inelastic": indeed, its limit

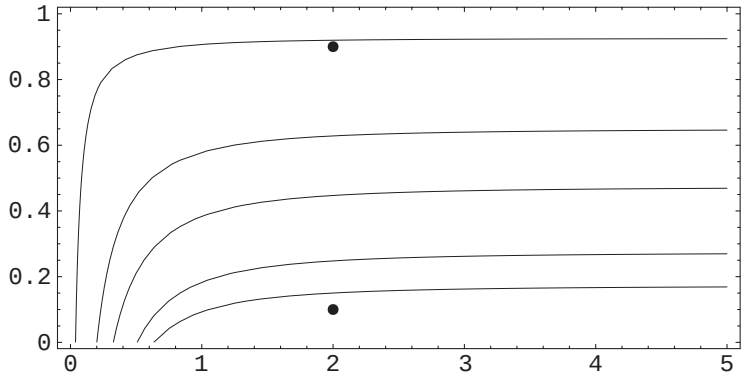

Fig. 1. – Contour plot of the maximum penetration depth $D_{\max}$ as a function of phenomenological parameters a (abscissa) and b (ordinate). The contour values of $D_{\max}$ are (top to bottom) 4.0, 4.5, 5.0, 6.0 and 7.0. The dots mark the two pairs of parameter values used in fig. 3.

value for $z \to -\infty$ is necessarily zero and only an exponential decay with depth is allowed. To overcome these limitations, here we consider a buoyancy frequency of the kind

$$B(z) = \sqrt{b + (1-b)\exp[a\,z]}\ , \tag{25}$$

where $a > 0$ and $0 \leq b \leq 1$. For a nonzero b, eq. (25) yields a profile of standard density that asymptotically (*i.e.* for great depths) increases linearly with depth, which is in agreement with measured data.

Obviously, the two previous cases correspond to $b = 1$ and $b = 0$, respectively; but, in general, we have $B(-\infty) = \sqrt{b} > 0$. Moreover, the Padé approximation of order (0,1)

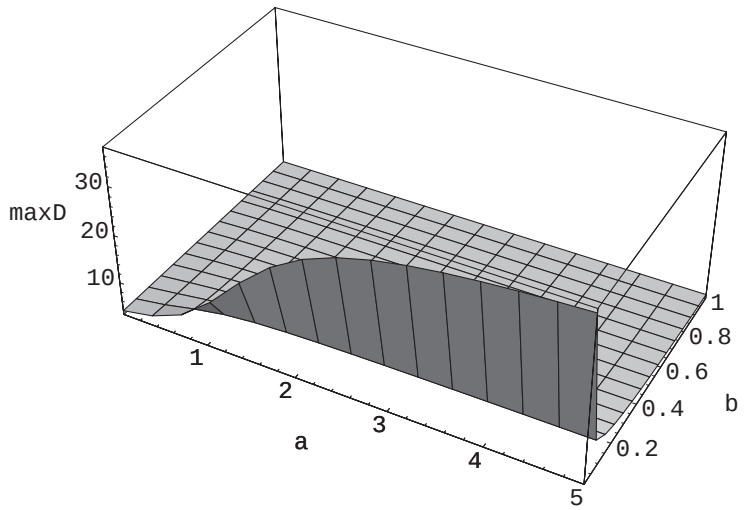

Fig. 2. – 3D plot of the maximum penetration depth $D_{\max}$ as a function of phenomenological parameters a and b.

of $B(z)$ at $z = 0$ is

$$\tilde{B}(z) = \frac{2}{2 - a\,(1-b)\,z}\ , \tag{26}$$

which shows that our family of functions (25) also encompasses, in some sense, the hyperbolic profile used, *e.g.*, in [9] and [10]. By means of ansatz (25), we are able to take into account both the location of the pycnocline (through parameter a), and a prescribed nonzero value of $B(z)$ at the bottom (through parameter b). Note that (25) satisfies both (2) and (3).

Assuming (25), we obtain

$$\Gamma(D) = -\left(\frac{1-b}{a^2}\right) - \frac{b}{2}\,D^2 + \frac{1-b}{a}\left(\frac{1}{a} + D\right) e^{-a\,D} \tag{27}$$

and hence

$$\Sigma(D) = \frac{1-b}{a^2}\left(\frac{-2}{a} + D\right) + \frac{b}{6}D^3 + \frac{1-b}{a^2}\left(\frac{2}{a} + D\right) e^{-a\,D}\ . \tag{28}$$

At this point we substitute (28) into (24) and find numerically $D_{\max}$ as a function of phenomenological parameters a and b. This new result, given by $D_{\max}(a,\, b)$ on the basis of (25), is represented as a contour plot in fig. 1, and as a three-dimensional plot in fig. 2: it is a continuous surface joining the two special cases found in the literature, *i.e.* $D_{\max}(a,\, 0)$ and $D_{\max}(a,\, 1)$. The square of the buoyancy frequency (25) is a convex linear combination of the above-mentioned special cases, and therefore all intermediate values may be retrieved. An interesting feature of these figures is that $D_{\max}(a, b)$ is almost constant with respect to a, if a is large enough (say, $a > 2$). Accordingly, if the pycnocline is sufficiently close to the free surface (or, better, to the interface between the upper Ekman layer and the geostrophic interior), then the maximum penetration depth of the motion is independent of the exact depth of the pycnocline, which is governed by parameter a. We also note a rapid increase of $D_{\max}(a, b)$ for b close to zero and a large enough. This behaviour is linked to the barotropic limit, in which the constancy of fluid density implies $D_{\max} = \infty$. In fact, the standard density is constant if and only if $B(z) \equiv 0$. But, because of (25), the condition $B(z) = 0$ for all negative z implies $b = 0$ and $a = \infty$. Thus, for small b and larger and larger values of a, the maximum penetration depth diverges to infinity.

4˙2. *Numerical examples.* – Starting from (21) with $\Sigma(D)$ given by (28) and the boundary condition (12), we can evaluate the no-motion interface $D(x, y)$. We have assumed, as it is most usual, a vertical Ekman current $w_{\mathrm{E}} = -\pi * \sin(\pi\, y)$. Moreover, (10) and (25) yield

$$\psi = \frac{b\,(1-y)\,(D+z)^2}{2} + \frac{(b-1)\,(y-1)\,\left(e^{-(a\,D)} + e^{a\,z}\,(-1 + a\,(D+z))\right)}{a^2}\ . \tag{29}$$

To visualize the structure of the so-obtained stream function, we select $B(z)$ by fixing $a = 2$ and letting $b = 0.1,\ 0.9$, and in fig. 3 we plot the related streamlines at the depths $z = -1,\ -3$.

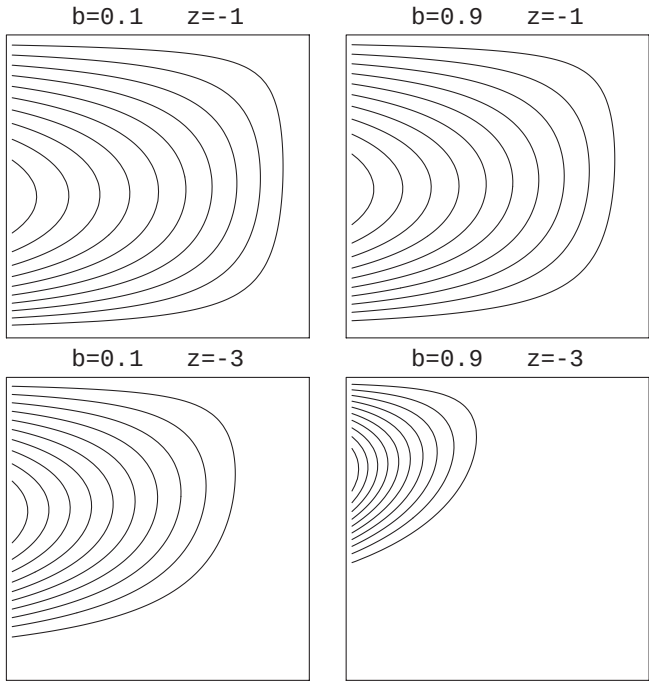

Fig. 3. – Contour plots of the stream function ψ given by eq. (40) with $a = 2.0$, and $D = D(x, y)$ obtained by numerically solving eq. (31).

The upper panels of fig. 3 show that the horizontal circulation pattern close to the free surface (say, for $z = -1$) is almost insensitive to the details of the buoyancy profile. This fact is consistent with the previous discussion leading to (23) and concerning with the linearization of $B(z)$ for z close to zero. On the other hand, at significantly greater depths (say, for $z = -3$), the streamlines strongly depend on the buoyancy profile, as it appears from the lower panels of fig. 3.

According to figs. 1 and 2, $D_{\max}$ is very high if $b = 0.1$ and very small if $b = 0.9$, given that $a = 2$ in both cases. Correspondingly, the flow structure tends to remain almost unaltered for $b = 0.1$ (left panels of fig. 3). But, the gradient of $D(x, y)$ depends on b because of (25) and is higher for lower b. Therefore, the moving fluid is squeezed towards the northwestern corner of the basin when $b = 0.9$ (right panels of fig. 3).

5. – Conclusion

In the framework of the Young and Rhines theory of the baroclinic wind-driven circulation, we have obtained some general results about the interface of no motion, which is a distinctive feature of the model with continuous stratification.

A special aspect of the theory, *i.e.* the maximum penetration depth of the interface, has been explored on the basis of weak assumptions about the vertical Ekman current and with the aid of a realistic two-parameter buoyancy frequency. Moreover, some of the above results have been confirmed through numerical examples of circulation forced by the usual sinusoidal Ekman current.

In our opinion, the model described in sect. **2** can give interesting hints also about some aspects of the ocean climate. Indeed, the basic inputs of the model, *i.e.* $B(x)$ and $w_{\mathrm{E}}(x, y)$, can be considered as slowing varying quantities that reflect interesting features of Earth's history. For instance, the buoyancy profile is sensitive to the density field, which is influenced by the unsteady temperature-salinity battle due to the competitions between evaporation and rainfall at low latitudes, and between colder temperatures and melted ice at high latitudes. On the other hand, the spatial distribution of the wind forcing also depends on the dynamics of the atmosphere through the feedback induced by the sea surface temperature. It is well known (*e.g.*, [11]) that NAO has a stochastic influence on the vertical current w_{E}, which, in turn, induces the reaction of the ocean currents against the slowly varying Ekman pumping.

Appendix A.

Mathematical properties of the interface of no motion

The aim of this Appendix is threefold: i) to obtain the nondimensional Ekman vertical velocity w_{E} in the form (13); ii) to prove that $D(x, y)$ is a decreasing and concave function of x; iii) to establish that the interface of no motion is unique.

i) The nondimensional Ekman vertical velocity is expressed by eq. (5) in terms of the Jacobian $J(\psi, \partial\psi/\partial z)$, which, in turn, may be computed at a generic depth z by resorting to (9) and (10). The result is

$$J\left(\psi, \frac{\partial\psi}{\partial z}\right) = (1-y)\, B(z)^2\, \frac{\partial D}{\partial x} \int_{-D}^{z} (\theta - z) B(\theta)^2 \,\mathrm{d}\theta \,. \tag{A.1}$$

On $z = 0$, eq. (A.1) simplifies into

$$J\left(\psi, \frac{\partial\psi}{\partial z}\right) = B(0)^2\, (1-y)\, \frac{\partial D}{\partial x}\, \Gamma(D) \qquad \text{on} \quad z = 0 \,,$$

where $\Gamma(D)$ is given by (14). Thus, eq. (5) becomes (13) because of (2).

ii) Equation (20) yields

$$\frac{\mathrm{d}D}{\mathrm{d}x} < 0 \qquad \forall x < 1 \,, \tag{A.2}$$

because M is positive and Γ is negative. Hence, D decreases with x. In particular, because of (12), we have $\Gamma(D(1)) = 0$; so that (20) yields

$$\lim_{x \to 1} \frac{\mathrm{d}D}{\mathrm{d}x} = -\infty \,,$$

whatever the nondimensional buoyancy frequency $B(z)$ may be.

From (20) we also deduce that $\mathrm{d}^2D/\mathrm{d}x^2 = -(M\, B^2\, D)/\Gamma(D)^2$, whence we see that in a subtropical gyre (where $M > 0$), we have $\mathrm{d}^2D/\mathrm{d}x^2 \leq 0$: this means that the interface $-D(x)$ is convex for every $B(z)$.

iii) Finally, we prove by contradiction that the solution of problem (20), (12) is unique. In fact, if $D_1(x)$ and $D_2(x)$ were two different solutions, and $D_1(x_0) \neq D_2(x_0)$ for a suitable x_0, then (21) would give both $\Sigma(D_1) = (1-x_0)\,M(y)$ and $\Sigma(D_2) = (1-x_0)\,M(y)$. These two equations would imply $\int_{D1}^{D2} \Gamma(D)\,\mathrm{d}D = 0$, but this integral cannot be zero, as the integrand is everywhere negative.

REFERENCES

[1] Ekman V. W., *Arkiv. Mat. Astron. Fys.*, **2** (1905) 11.
[2] Sverdrup H. U., *Proc. Nat. Acad. Sci.*, **33** (1947) 318.
[3] Charney J. G., *J. Mar. Res.*, **14** (1955) 477.
[4] Young W. R. and P. B. Rhines, *J. Mar. Res. (Suppl.)*, **40** (1982) 559.
[5] Young W. R. and P. B. Rhines, *J. Mar. Res.*, **40** (1982) 849.
[6] Young W. R., *Baroclinic theories of the wind driven circulation*, in *General Circulation of the Ocean*, edited by H. D. I. Abarbanel and W. R. Young (Springer-Verlag) 1987, pp. 134-201.
[7] Pedlosky J., *Ocean Circulation Theory* (Springer-Verlag) 1996.
[8] Garrett C. J. R. and W. H. Munk, *Geophys. Fluid Dyn.*, **3** (1972) 225 (cited in Le Blond P. H. and L. A. Mysak, *Waves in the Ocean* (Elsevier) 1978).
[9] Balmforth N. J. and W. R. Young, *J. Mar. Res.*, **57** (1999) 561.
[10] Gill A. E., *J. Phys. Oceanogr.*, **14** (1984) 1129.
[11] Dewar W. K., *J. Clim.*, **14** (2001) 4380.